AGU PUBLICATIONS

JGR

Journal of Geophysical Research: Earth Surface

RESEARCH ARTICLE
10.1002/2016JF003876

Key Points:
- Seasonal soil freeze/thaw state is sensitive to climate change
- The area extent of soil completely frozen state is in decreasing with warming climate
- Soil freeze/thaw cycle is highly correlated with air temperature

Correspondence to:
T. Zhang,
tjzhang@lzu.edu.cn

Citation:
Peng, X., O. W. Frauenfeld, B. Cao, K. Wang, H. Wang, H. Su, Z. Huang, D. Yue, and T. Zhang (2016), Response of changes in seasonal soil freeze/thaw state to climate change from 1950 to 2010 across china, *J. Geophys. Res. Earth Surf.*, *121*, 1984–2000, doi:10.1002/2016JF003876.

Received 8 MAR 2016
Accepted 5 OCT 2016
Accepted article online 8 OCT 2016
Published online 4 NOV 2016

Response of changes in seasonal soil freeze/thaw state to climate change from 1950 to 2010 across china

Xiaoqing Peng[1,2], Oliver W. Frauenfeld[2], Bin Cao[1,3], Kang Wang[4], Huijuan Wang[1], Hang Su[1], Zhe Huang[1], Dongxia Yue[1], and Tingjun Zhang[1]

[1]Key Laboratory of Western China's Environmental Systems (Ministry of Education), College of Earth and Environmental Sciences, Lanzhou University, Lanzhou, China, [2]Department of Geography, Texas A&M University, College Station, Texas, USA, [3]Department of Geography and Environmental Studies, Carleton University, Ottawa, Ontario, Canada, [4]Institute of Arctic and Alpine Research, University of Colorado Boulder, Boulder, Colorado, USA

Abstract Variations in seasonal soil freeze/thaw state are important indicators of climate change and influence ground temperature, hydrological processes, surface energy, and the moisture balance. Previous studies mainly focused on the active layer and permafrost, while seasonally frozen ground research in nonpermafrost regions has received less attention. In this study, we investigate the response of changes in seasonal soil freeze/thaw state to changes in air temperatures by combining observations from more than 800 stations with gridded mean monthly air temperature data across China. The results show that mean annual air temperature (MAAT) increased statistically significantly by 0.29 ± 0.03°C/decade from 1967 to 2013, with greater warming on the Qinghai-Tibetan Plateau. There is a statistically significant decrease in the freeze/thaw cycle (FTC) at 0.39 ± 0.05 cycles/decade. In addition, there are strong negative correlations between FTC and MAAT. Estimating the soil freeze/thaw state classification based on the number of days in the month, we find that changes of mean annual area extent of seasonal soil freeze/thaw state decreased significantly for completely frozen (CF) ground, while the area extent of partially frozen (PF) and unfrozen (UF) ground both increased. Changes in mean monthly area extent of seasonal soil freeze/thaw state indicate that the extent of CF and UF area was decreasing and increasing, respectively. But for the extent of PF areas, both increasing and decreasing trends were observed. Quantifying the spatial pattern of the seasonal soil freeze/thaw, we find that CF and PF areas are located in northern China and the Tibetan Plateau from December to March, and UF areas are located in southern China. The variations of mean annual area extent departure of soil freeze/thaw states are consistent with MAAT changes in different land cover types across China.

1. Introduction

The globally averaged combined land and ocean surface temperature rose 0.85 (0.65 to 1.06)°C from 1880 to 2012 according to the Intergovernmental Panel on Climate Change (IPCC) [*Stocker et al.*, 2014]. It is very likely that the number of cold days and nights has decreased, and the number of warm days and nights has increased on the global scale [*Stocker et al.*, 2014]. Concurrent with global warming, the seasonal soil freeze/thaw state was also affected, as the annual soil freeze/thaw state is well coupled to the land surface energy and moisture fluxes, and plays a key role in the climate system. Change of soil freeze/thaw state can also significantly affect landscapes, ecosystems, and hydrological processes [*Zhang and Armstrong*, 2001; *Zhang et al.*, 2003; *Jorgenson et al.*, 2006; *Gruber and Haeberli*, 2007; *Frauenfeld and Zhang*, 2011; *Wang et al.*, 2015].

Changes of seasonal soil freeze/thaw state have an important effect on carbon exchange between the atmosphere and the ground. Frozen organic soils potentially contain more than twice the amount carbon currently in the atmosphere [*Tarnocai et al.*, 2009; *Mu et al.*, 2015]. Permafrost thaw and seasonal soil freeze/thaw processes may result in exposure of previously frozen carbon to microbial degradation and release radiatively active gases such as carbon dioxide (CO_2) and methane (CH_4) into the atmosphere [*Zimov et al.*, 2006; *Schuur et al.*, 2009; *Wang et al.*, 2009, 2014; *Zhang et al.*, 2014; *Song et al.*, 2014; *Mu et al.*, 2015].

The seasonal soil freeze/thaw state can influence hydrological processes, whereby the increasing thaw depth leads to a decrease in surface runoff [*Wang et al*., 2014]. Soil freeze/thaw affects the soil water storage capacity, soil water infiltration capacity, and hydraulic conductivity and leads to a redistribution of water in the soil profile. Consequently, seasonal variations in soil freeze/thaw state are the main cause for seasonal changes in groundwater discharge and subsequent surface runoff [*Wang et al*., 2014]. Many previous studies have reported the impact of soil freeze/thaw on surface runoff [*Kuchment et al*., 2000; *McGuire et al*., 2002; *Miyazaki et al*., 2014; *Yamazaki et al*., 2006]. The influences are most evident in Arctic permafrost regions, because of the pronounced soil freeze/thaw cycle and the presence of frozen soil [*Hayashi et al*., 2003; *McNamara et al*., 1998; *Streletskiy et al*., 2015].

Most previous research focused on either the point scale or the regional scale. Point-scale studies emphasize the timing and durational of the soil freeze state, such as freeze days, freeze/thaw cycle, and the freeze depth [*Frauenfeld et al*., 2004; *Zhang et al*., 2014; *Wang and Zhang*, 2013; *Henry*, 2007; *Sinha and Cherkauer*, 2008; *Anandhi et al*., 2013; *Wang et al*., 2015]. For example, *Wang et al*. [2015] used 1956–2006 ground surface temperature data from 636 observational sites to analyze changes in the timing and duration of the near-surface soil freeze/thaw status. Results indicated that overall during the study period, the first date of the near-surface soil freeze was delayed by about 5 days in autumn, while the last date was advanced by about 7 days in spring. As a result, the duration of the near-surface soil freeze was reduced by about 12 days, while the actual number of the freeze day decreased about 10 days. However, *Wang et al*. [2015] mainly conducted trend analysis using time series at individual stations and a composite time series using data from 636 stations across China. The regional scale employs satellite remote sensing techniques, such as passive and active microwave remote sensing. The main passive sensors generally used for this are the scanning multichannel microwave radiometer, Special Sensor Microwave Imager, Advanced Microwave Scanning Radiometer (AMSR), and the enhanced version, AMSR-E [*Zhang and Armstrong*, 2001; *Zhang et al*., 2003, 2004; *Smith*, 2004; *Zhang et al*., 2009, 2011; *Li et al*., 2012; *Jin and Li*, 2002; *Jin Rui and Tao*, 2009; *Jin et al*., 2015; *Zhao et al*., 2009], while synthetic aperture radar is the primary active sensor [*Way et al*., 1994; *Zhang et al*., 2004; *Liu et al*., 2010, 2012; *Chen et al*., 2013]. However, on the regional scale, the spatial resolution is still very coarse, and satellite products are not well suited for areas where the surface is heterogeneous. This is particularly important for soil freeze/thaw detection, because it is strongly affected by such heterogeneous surface conditions. Especially in complex terrain, remote sensing methods are very limited.

In *Peng et al*. [2016], we employed the Stefan solution to investigate soil seasonal freeze depth in nonpermafrost regions across China using daily air temperature from 839 stations, soil temperature measured at 11 depths ranging from 0 cm to 320 cm from 845 stations, and monthly gridded air temperature. Results demonstrate that the soil freeze depth decreased significantly, at −0.18 cm/year from 1967 to 2012, with a net change of about 8.05 cm at the 839 sites. The spatial variability of soil freeze depth ranges between 0.0 and 4.5 m across China. Air temperature, thawing index, and vegetation growth are significantly negatively correlated with soil freeze depth, but no correlation exists between snow depth and soil seasonal freeze depth [*Peng et al*., 2016]. While the *Peng et al*. [2016] study mainly focused on estimating the depth of seasonal soil freeze, the near-surface (approximately 5 cm) soil freeze/thaw status is likely more directly related to the overlying atmosphere and thereby critical for energy and moisture exchanges between the soil and the atmosphere, plant growth, agriculture, and ecosystems as a whole. This near-surface soil freeze/thaw status is therefore the focus of our current study. To improve the data resolution and consider land cover impacts on soil freeze/thaw state, we classify soil freeze/thaw status for different land cover types using more than 800 sites, to establish the relationship between monthly freeze days and mean monthly air temperature. Because of the complex terrain and spatial heterogeneity across China, this approach should improve the accuracy of soil freeze/thaw state classification. Unlike prior studies that used only point measurements [e.g., *Wang et al*., 2015], we use a combination of station observations, gridded data, and satellite remote sensing land cover type products to estimate seasonal soil freeze/thaw state in the complex terrain of China. Here we define soil freeze/thaw status according to temperature only and do not explicitly consider soil moisture. The specific goals are as follows:

1. To assess the spatial and temporal variations of the near-surface soil seasonal freeze/thaw status from 1950 to 2010 across China, incorporating a land cover classification. This is the first time that the seasonal soil freeze/thaw state has been considered in conjunction with different land cover types.

2. To quantify the variability of the daily near-surface soil freeze-thaw cycle until 2013.
3. To investigate the response of variations in seasonal soil freeze/thaw status to climate change across China.

2. Data and Methods

2.1. Data

We analyze temperature changes and the seasonal soil freeze/thaw status for China using four types of temperature data: (1) daily air temperature, (2) daily ground surface temperature, (3) mean monthly gridded air temperature, and (4) daily soil temperature at 5 cm depth. All temperature data were obtained from the China Meteorological Administration (CMA) except the gridded data. In addition, we use 1 km resolution digital elevation model (DEM) and land cover data. All data sets are described below.

2.1.1. Daily Air Temperature and Ground Surface Temperature

We obtained daily air temperature and daily ground surface temperature measurements for 839 stations located throughout China from the CMA (Figure 1). A number of standard procedures were applied by the CMA to improve data quality. Based on the metadata document from the CMA, the ground surface temperature is measured at 0 cm. This data set was used to calculate the mean monthly and annual temperature. The ground surface temperature was then also used to calculate the ground surface freeze days at 0°C. Some stations date back to the 1950s, and more than 800 began in the 1960s. While some station records end around the 1990s, others are available through 2013. The spatial distribution is such that most stations are located in east central China, and only a few sites are located in the west and in high-altitude areas such as the Qinghai-Tibetan Plateau (Figure 1). In this study, the daily air temperature is used to estimate temperature changes during 1967–2013 based on varying station numbers, ranging from 803 sites in 1967 to 839 sites in 2013.

2.1.2. The 5 cm Depth Soil Temperature

Daily soil temperature at 5 cm depth was used to calculate the soil freeze days at or below 0°C for 846 sites across China, obtained from CMA (Figure 1). The period of record at these locations varies, with some stations dating back to the late 1950s and some only to the 1970s. Some station records end around the 1990s, while others are available through 2006 [*Wang et al*., 2015]. There are a total of 729 locations that have daily air, ground surface, and soil temperature observations for this study.

2.1.3. Mean Monthly Gridded Air Temperature

Gridded air temperature was used to analyze soil freeze/thaw state at the regional scale across China. We obtained mean monthly gridded air temperature (MMGAT) from the Terrestrial Air Temperature 1900–2010 Gridded Monthly Time Series product (http://climate.geog.udel.edu/~climate/), with $0.5° \times 0.5°$ spatial resolution. This data set was produced by combining many observational station records over the world, using a spatial interpolation method and spatial cross-validation process [*Legates and Willmott*, 1990; *Peterson and Vose*, 1997; *Peterson et al*., 1998; *Willmott et al*., 1985; *Willmott and Matsuura*, 1995; *Willmott and Robeson*, 1995]. In this research, the period 1950–2010 was chosen to analyze the seasonal soil freeze/thaw state across China.

2.1.4. Digital Elevation Model

Considering the impacts of elevation and the complex terrain across China on air temperature, we also used the GTOPO30 (https://lta.cr.usgs.gov/GTOPO30) digital elevation model (DEM) data in this study to further improve the monthly gridded air temperature data resolution. GTOPO30 was derived from several raster and vector sources of topographic information and has a 30 arc sec resolution. Across China, the elevation ranges from −152 to 8752 m (Figure 1). Based on the DEM data, we spatially interpolate the monthly gridded air temperature data to 1 km resolution.

2.1.5. Land Cover Data

Land cover changes can influence local and regional climate by modifying the surface energy, water, and momentum fluxes, as well as greenhouse gases. These changes can influence the soil freeze/thaw state [*Ran et al*., 2010]. Thus, classifying soil freeze/thaw status for our analysis will be based on the land cover product version 2.0 from the West Data Center (http://westdc.westgis.ac.cn/), with 1 km spatial resolution in 2000 [*Ran et al*., 2010] based on the International Geosphere-Biosphere Program land cover classification system and its 18 types (Table 1). Based on *Zhang et al*. [2005], we merged classes 1 to 9 as forest, type 12 and 14 as cropland, and type 16 and 18 as barren or sparsely vegetated. As a result, there are six classes (not counting

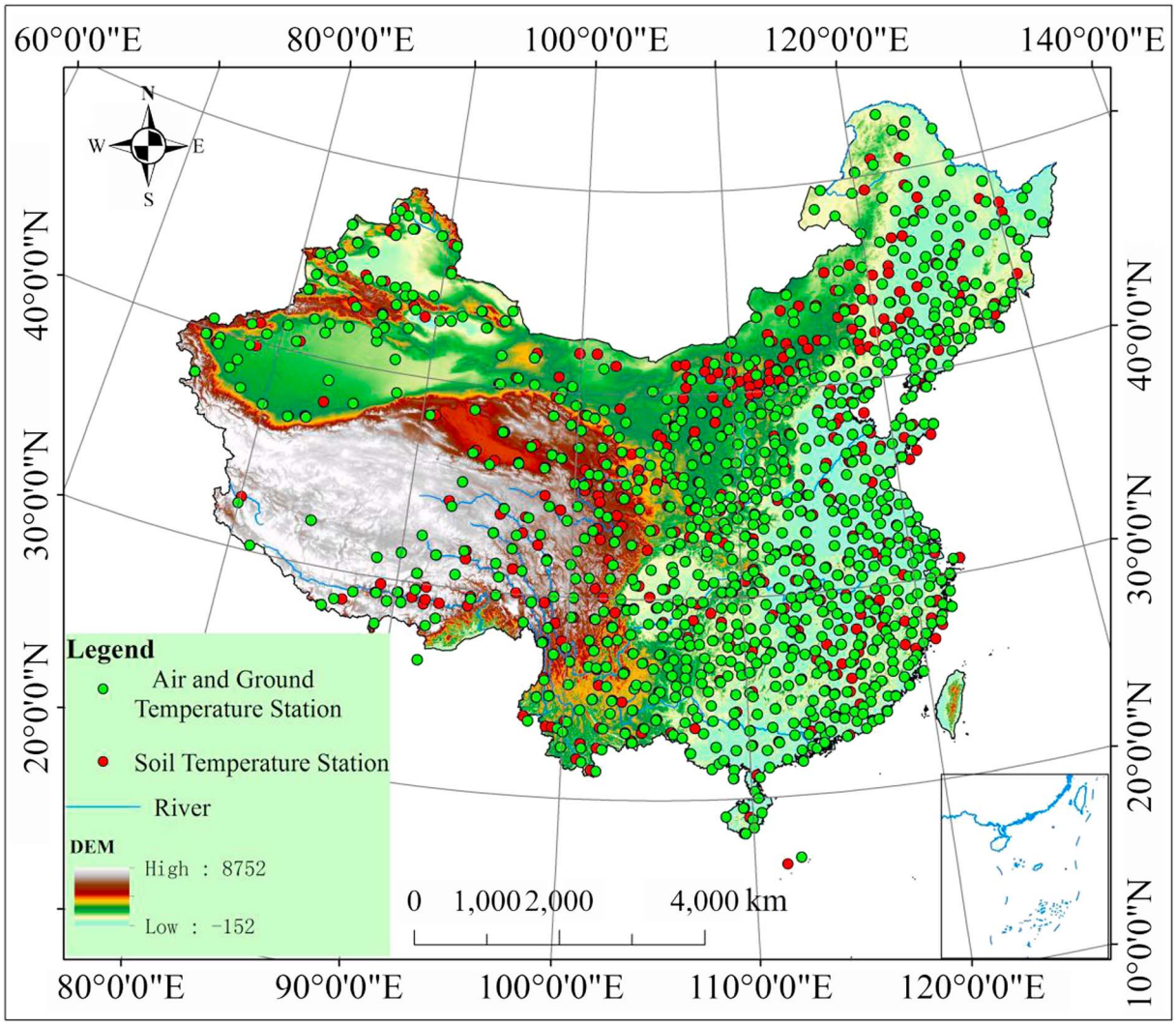

Figure 1. Map showing the location of soil temperature and air temperature stations available across China. The 845 green points represent the air and ground surface temperature station. The 839 red points represent the soil temperature station. The color shading corresponds to surface elevation.

water bodies or snow and ice) used here (Figure 2). This static land cover product from 2000 is used in our paper for classifying soil freeze/thaw states. While land cover in general has, of course, changed across China, the surface cover at the meteorological stations is preserved over time and has therefore remained relatively consistent. Nonetheless, this is an important caveat to our results.

2.2. Methods

Missing data often present a potential problem for analyzing and averaging time series. Therefore, if fewer than 5 days were missing in a given month, filling in missing daily air temperatures was based on highly correlated neighboring sites using linear regression. Missing daily mean ground surface temperatures were estimated through linear regression with the daily mean air temperature at the same station. Based on the daily air temperature, we also calculate the mean monthly air temperature. The monthly lapse rate is estimated by the monthly air temperature and elevation of observational sites across China. The monthly lapse rate is subsequently used for producing the 1 km resolution MMGAT.

To derive a 1 km resolution MMGAT from $0.5° \times 0.5°$ data, spatial interpolation was used in conjunction with the 1 km resolution DEM. Incorporating elevation influences through an average air temperature lapse rate can increase the accuracy of spatially interpolated average air temperature [*Willmott and Matsuura*, 1995].

Table 1. International Geosphere-Biosphere Programme Land Cover Classification System

Number	Class Name
1	Evergreen Needleleaf Forests
2	Evergreen Broadleaf Forests
3	Deciduous Needleleaf Forests
4	Deciduous Broadleleaf Forests
5	Mixed Forests
6	Closed Shrublands
7	Open Shrublands
8	Woody Savannas
9	Savannas
10	Grasslands
11	Permanent Wetlands
12	Croplands
13	Urban and Builtup Lands
14	Cropland/Natural Vegetation Mosaics
15	Snow and Ice
16	Barren
17	Water Bodies
18	Bare Soil

The data processing steps are to (1) bring each average monthly gridded air temperature to sea level using the average monthly lapse rate calculated at the meteorological stations, (2) apply the traditional interpolation to the adjusted-to-sea-level average-monthly gridded air temperatures, and (3) bring the gridded sea-level air temperature back to the DEM-gridded height. Based on the more than 800 sites, we test the interpolated MMGAT and observational monthly air temperature and find that the regression coefficient is generally 1.0, with a minimum of 0.98 in April.

We calculated the FD, from the daily mean soil temperature at 5 cm depth,

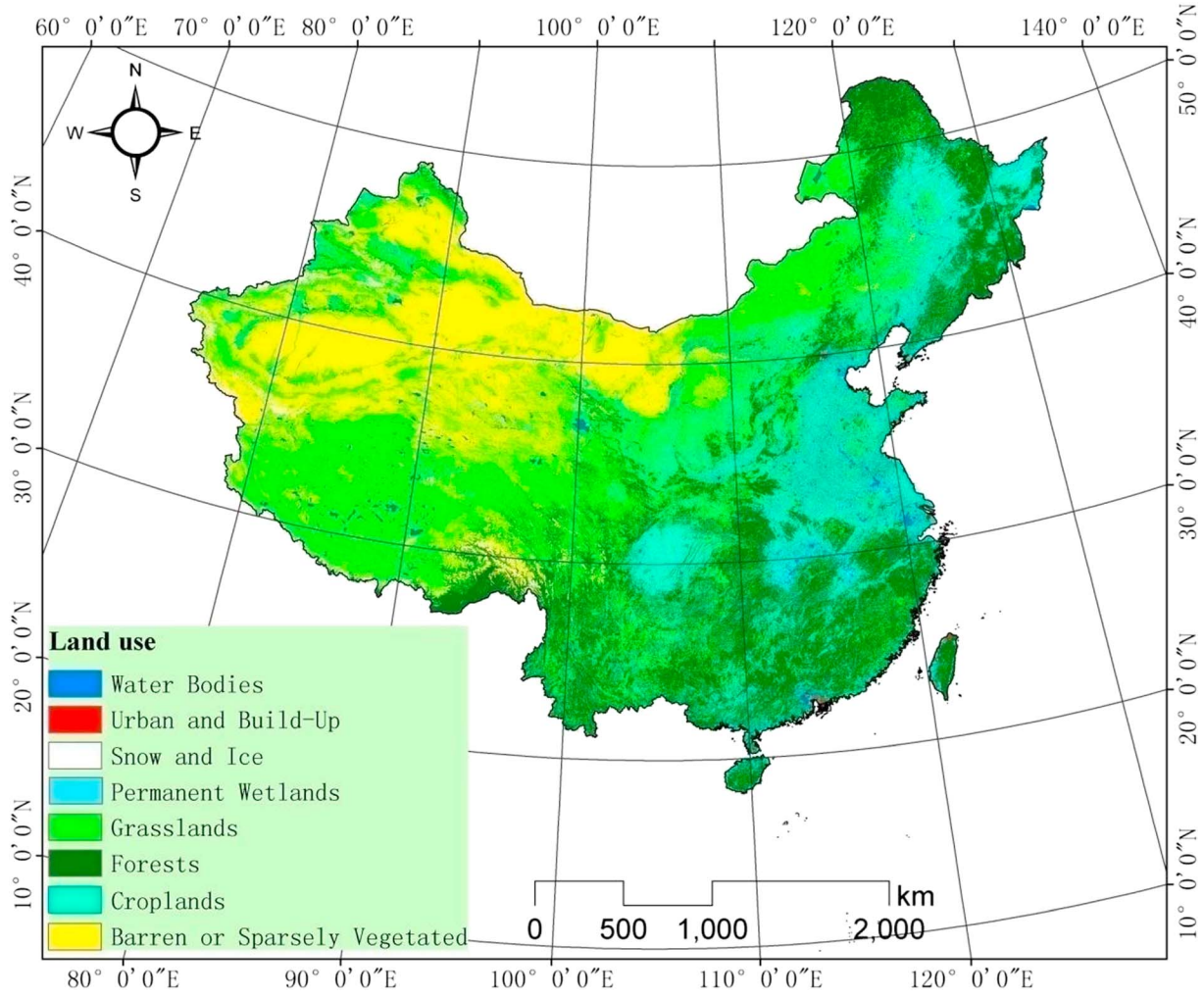

Figure 2. Spatial distribution of land cover in 2000 across China based on the land cover product version 2.0 from the West Data Center.

based on when temperatures are at or below 0°C. We define a daily ground surface freeze/thaw cycle (FTC) if the daily mean ground surface temperature switches from positive to negative temperature, or vice versa, in the course of 1 day [*Guo et al*., 2011; *Henry*, 2007; *Zhang et al*., 2003]. FTC estimated from daily ground surface temperature is used to explore the relationship with MAAT. FD estimated from daily soil temperature at 5 cm depth is used to analyze the seasonal soil freeze/thaw state.

For the seasonal soil (at 5 cm depth) monthly freeze/thaw status, we define three classes (equation (1)): completely frozen (CF), when the soil is frozen for the entire month, i.e., the freeze days equal the total number of days in the month; partially frozen (PF), when the soil layer experiences both freeze and thaw, meaning that the number of freeze days is less than the number of days in the month, but greater than zero; and unfrozen (UF), when the soil is thawed for the entire month, and the number of freeze days is thus zero in the month [*Peng et al*., 2013].

$$\mathrm{FD} = \begin{cases} = 30 & \mathrm{CF} \\ 0 < \mathrm{FD} < 30 & \mathrm{PF} \\ = 0 & \mathrm{UF} \end{cases} \quad (1)$$

In equation (1), a number of 30 days per month are used. We establish the relationship between mean monthly air temperature (MMAT) and FD in each land cover type based on this method.

To characterize contemporary or recent climate change, high-quality observed climatological data are required for a baseline period. The most widely used climatological baseline period is the nonoverlapping 30 year "normal" period, as defined by the World Meteorological Organization. We use 1971–2000 as the baseline [*Stocker et al*., 2014] to calculate the temporal trends of seasonal soil freeze/thaw area extent in each freeze/thaw category, estimate temperature changes, and the FTC departures.

Linear regression and spatial analysis are used to analyze the trends of air temperature, FTC, and the monthly area extent of the three soil freeze/thaw states. Thus, the mean annual area extent of three different freeze/thaw states can be calculated based on the monthly area extent.

To quantify the spatial distribution of the seasonal soil freeze/thaw state, we assign the CF, PF, and UF status values of 1.0, 2.0, and 3.0, respectively, and calculate time series of the distribution of each soil freeze/thaw state in each month.

For the trend estimation and change point detection in the climatic series and freeze/thaw state area extent, we use the Pettitt and Mann-Kendall Change Point Test [*Bates et al*., 2012]. We choose a 95% confidence level to assess significance for all statistical analyses.

3. Results

3.1. Variability of Freeze/Thaw Cycle

The ground surface soil freeze/thaw state is coupled to the timing and duration of cold/warm seasons and is an important indicator of climate change [*Zhang et al*., 2001]. One of the most important factors is FTC, which could reflect the climate change indirectly.

Figure 3 shows the spatial distribution of the climatological (1971–2000) FTC and corresponding trends at each station. The spatial distribution of FTC seems to be mainly controlled by latitude and altitude. The highest values of FTC are on the Tibetan Plateau and across the northern reaches of China, and the smallest FTC vales are in the southeast. Declined statistically significant decreasing FTC trend is observed across China at 262 sites, with magnitudes of −2.0 and 0.0 frequency/decade. However, increases are also evident at 14 stations, ranging from 0 to 2.0 frequency/decade. Most of the significant FTC trends are negative across China.

FTC is one important factor influencing the ground surface soil freeze/thaw state. It indicates a potential climate change trend toward warming across China over recent decades.

3.2. Seasonal Soil Freeze/Thaw State

The extent of seasonal soil freeze/thaw is mapped using MMAT. To do so, a relationship between seasonal soil freeze/thaw state and MMAT needs to be established [*Zhang et al*., 2003]. Based on previous research, seasonal soil freeze/thaw is influenced by land cover [*Zhang et al*., 2005; *Jin et al*., 2015]. Excluding water bodies and

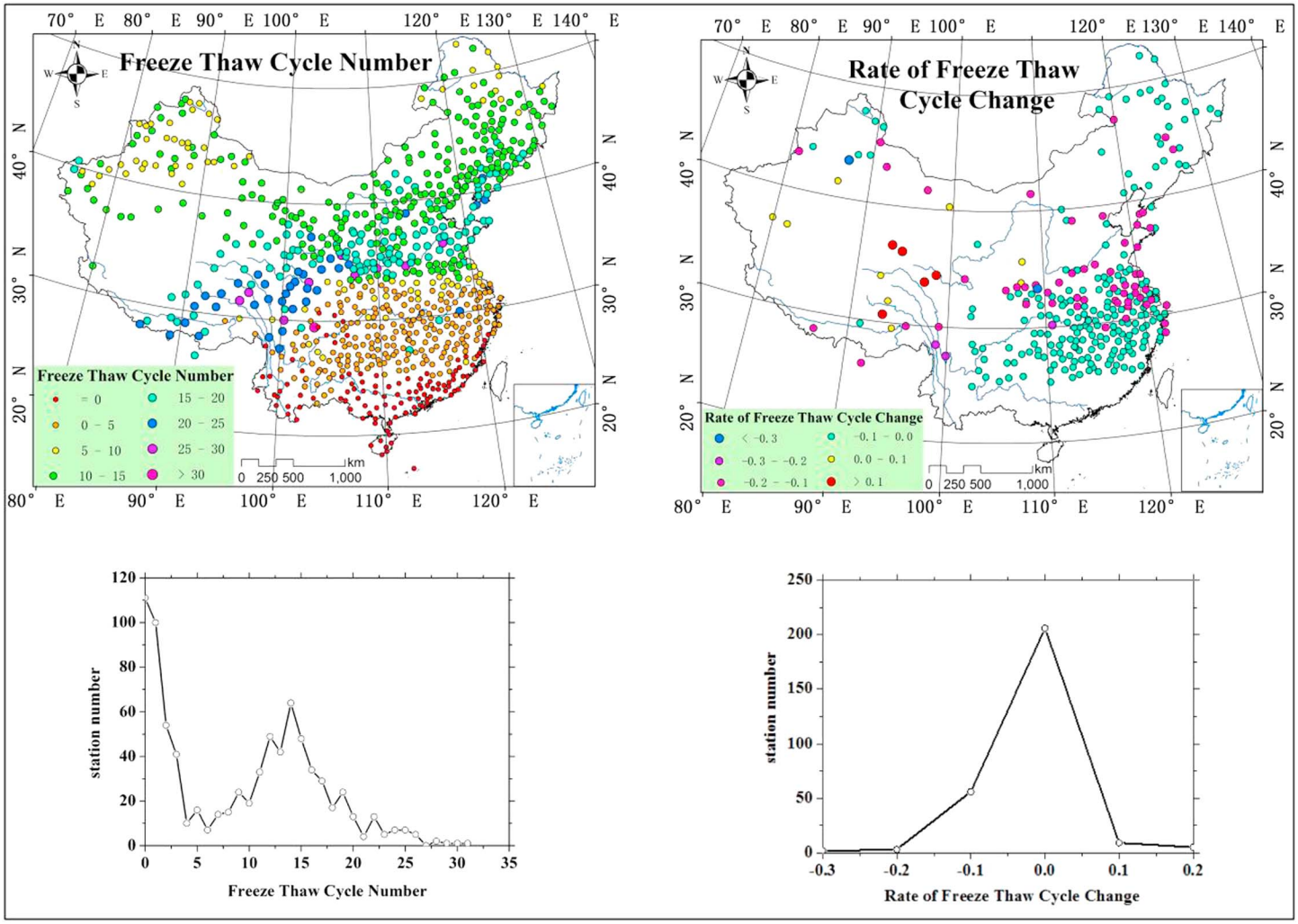

Figure 3. Spatial distribution of FTC with respect the 1971–2000 mean and the rate of FTC change at the meteorological stations across China. Only statistically significant ($p < 0.05$) trends in FTC are shown.

snow and ice, the relationship between MMAT and the total monthly number of soil freeze days at 5 cm depth in six different land cover classes was established.

Figure 4 shows the seasonal soil freeze/thaw state is different for different land cover types. Land cover types have distinct surface properties and albedos, thus have different interactions with air temperatures and the surface energy balance, and consequently have a different influence on the soil thermal regime. Taking croplands as an example, the temperature range of the seasonal soil PF state is determined as the zone between the −6.5°C and 5°C MMAT isotherms, and the temperature range of seasonal soil CF and UF states is determined as the zone below −6.5°C, and above 5°C MMAT, respectively. The temperature range of soil PF state is as follows: between −7 and 6°C for barren or sparsely vegetated, between −9 and 4°C for forests, between −8 and 4°C for grasslands, between −6 and 3.5°C for wetlands, and between −7 and 6°C for urban areas.

3.3. Spatial and Temporal Variations of Soil Freeze/Thaw State at 5 cm Depth

Based on the seasonal soil freeze/thaw divisions, mean monthly and annual area extent of every status can be estimated. Figure 5 represents time series of mean annual area extent of the 1950–2010 CF, PF, and UF soil freeze/thaw departures from their climatologic mean (1971–2000). Mean annual CF area extent decreased statistically significantly across China at a rate of 0.043×10^6 km^2/decade. In contrast, a significant increasing trend of 0.037×10^6 km^2/decade was found in area extent of soil UF state. Based on a change-point analysis, a

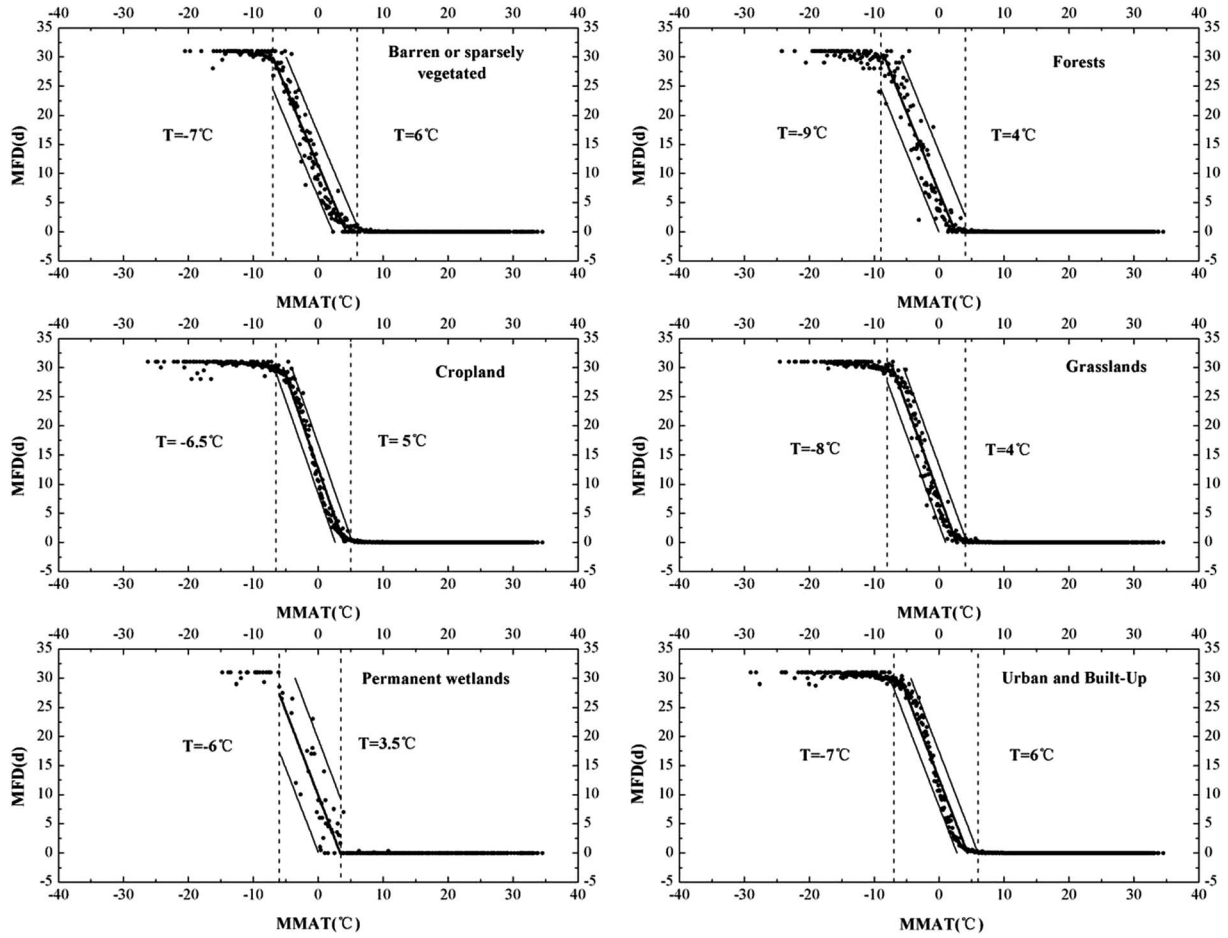

Figure 4. Relationship between mean monthly air temperature and monthly total number of soil freeze days at 5 cm depth at observational stations in different land cover types across China. The dotted lines in each figure are the monthly air temperature thresholds to classify the different soil freeze/thaw states.

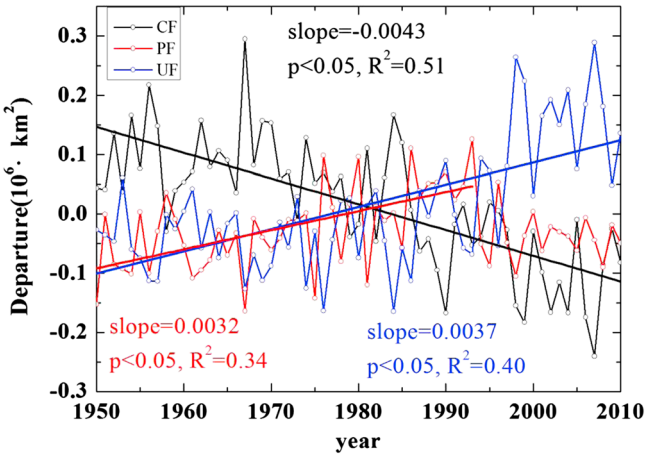

Figure 5. Variation of annual area extent of soil freeze/thaw states across China from 1950 to 2010. Black, red, and blue solid lines represent the area extent of soil CF, PF, and UF state, respectively. Also indicated are the trend analysis variables of slope, R^2, and p values.

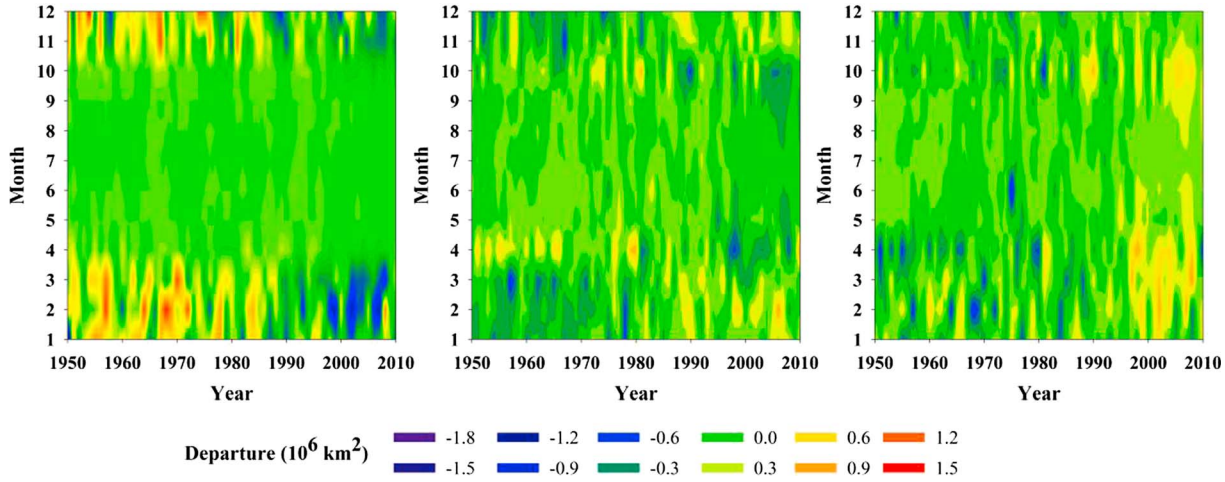

Figure 6. The 1950–2010 changes in monthly area extent of seasonal soil freeze/thaw states at 5 cm depth over China for (left) CF, (middle) PF, and (right) UF.

statistically significant increasing trend of 0.032×10^6 km^2/decade is evident in the area extent of PF state from 1950 to 1993, followed by no trend from 1994 to 2010. Mean annual area extent of soil CF and UF state exhibited much greater interannual variability and was more susceptible to outliers and leverage points. Overall, the increases of UF and decreases of CF area extent primarily reflect a temperature rise that influenced the soil freeze/thaw state.

Monthly area extent of soil freeze/thaw state shows substantial change from 1950 to 2010 across China (Figure 6). The CF state departure was positive, ranging between 0.6×10^6 km^2 and 0.9×10^6 km^2 from 1950 to 1985 in January, February, March, November, and December, and negative after 1985. This suggests that monthly area extent of soil CF state decreased statistically significantly in these months after 1985. In contrast, the monthly area extent departure was near zero in the other months, indicating no significant change. The winter area extent of soil PF state was negative before 1980 and positive thereafter. The lowest monthly area extent departure of -0.83×10^6 km^2 was in March 1957, and the maximum value of 0.83×10^6 km^2 occurred in April 2010. The monthly area extent of UF soil state shows negative values before 1957 in winter, spring, and autumn, and positive after 1995, even reaching 0.9×10^6 km^2 in some years. In summer, the values were most above zero, especially after 2000. Interannual variations of monthly area extent of soil freeze/thaw state also show significant trends (Figure 7). The CF soil change was negative in all months. This indicates that the monthly area extent of CF soil state decreased from 1950 to 2010, in

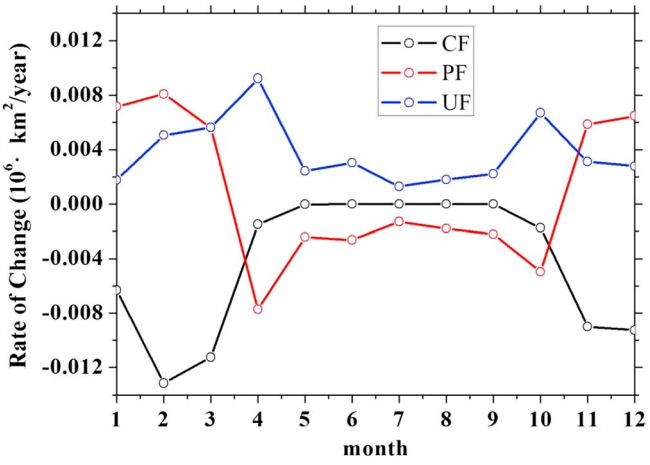

Figure 7. Spatial variations of mean monthly soil freeze/thaw values from 1950 to 2010 at 5 cm depth across China. CF state is arbitrarily assigned a value of 1.0, PF state as 2.0, and UF state as 3.0.

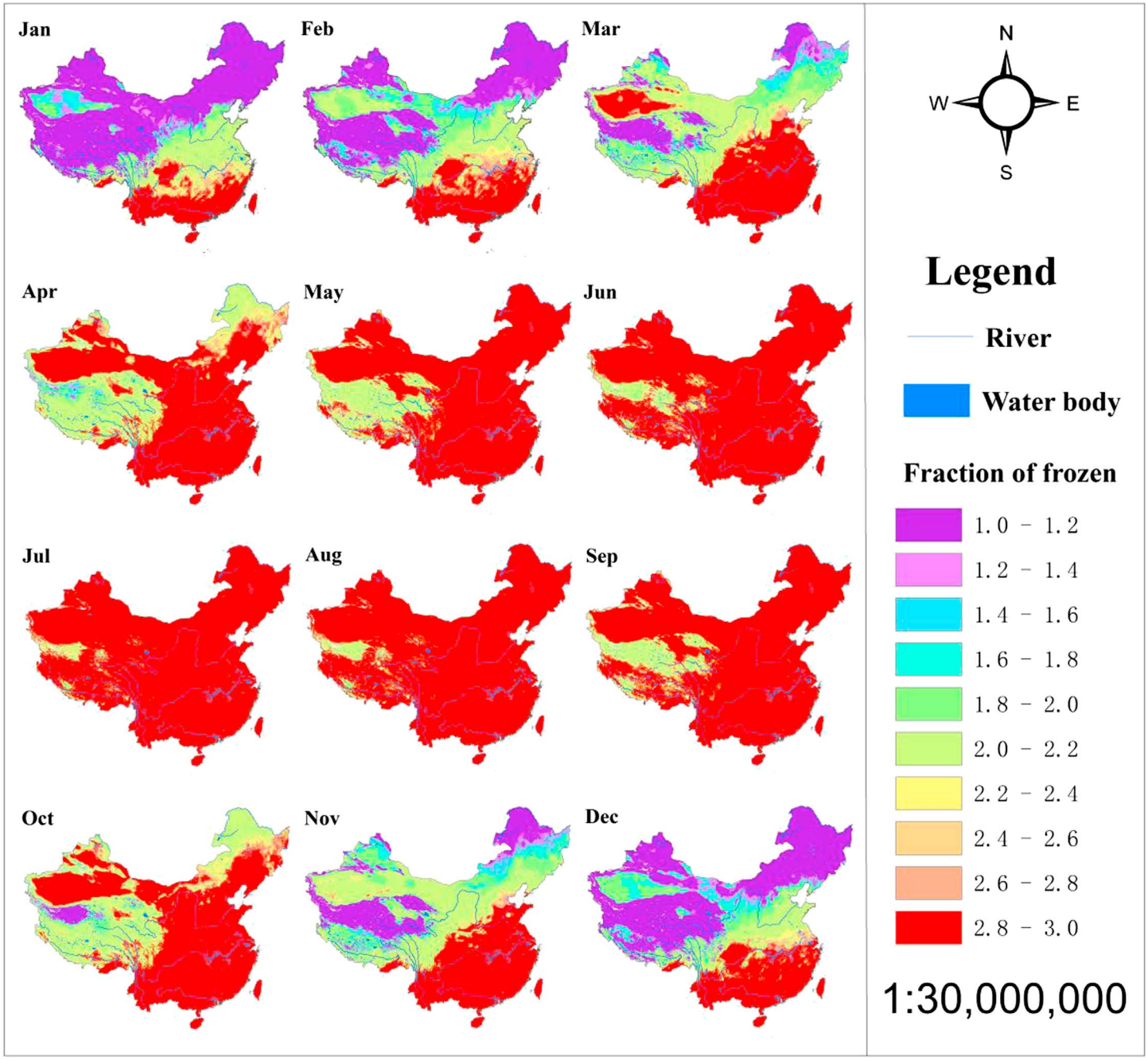

Figure 8. Variations of mean annual area extent of soil freeze/thaw state ((left column) CF, (middle column) PF, and (right column) UF) for different land use types from 1950 to 2010. The *y* axis is the land use type, where 1 is barren or sparsely vegetated, 2 is forests, 3 is croplands, 4 is grasslands, 5 is permanent wetlands, and 6 is urban and buildup.

contrast to the UF soil state which is positive during each month. During the warm season, from May to September, there was no variability in the changes of these states. PF values are negative from April to October, illustrating a decreasing trend of monthly area extent of this state. When it was positive, from November to March, this indicates an increasing trend in these months.

Figure 8 shows the spatial distribution of seasonal soil freeze/thaw state in each month. The areas with values less than 1.4 (primarily CF and PF) are mainly in the north of China and the Tibetan Plateau from December to March. The greatest values (UF) are primarily located in the south of China. From January to July, the fraction

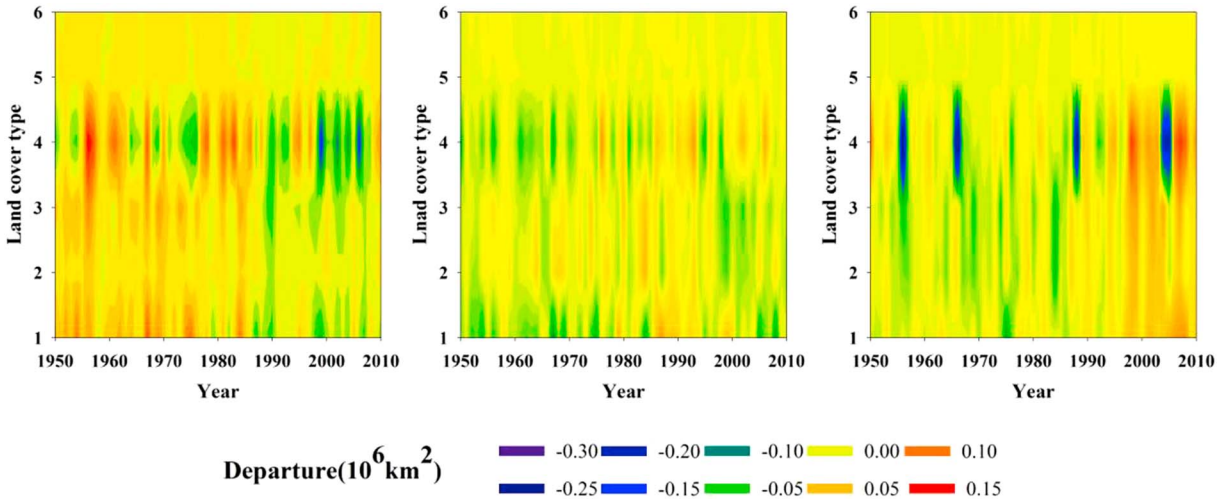

Figure 9. Time series and linear trends of MAAT departures for different land cover types from 1950 to 2010.

increased from 1.0 to 3.0 with a maximum in July, indicating a transition from CF to UF. However, the values decreased, and the area extent of lower values (CF and PF) increased from August to December. This distribution of CF, PF, and UF areas agrees well with the spatial and temporal variations of mean monthly soil freeze/thaw state.

3.4. Area Extent Variability of Soil Freeze/Thaw in Different Land Cover Types

Temperature directly influences soil freeze/thaw; however, the response of land cover to temperature is different. As in *Zhang et al*. [2005], we use land cover as the basis for classifying soil freeze/thaw states. Based on the land cover classification from 2000, we calculated the mean annual area extent departure of soil freeze/thaw state in different land cover types from 1950 to 2010 (Figure 9). Variations of mean annual area extent of soil CF state were similar in some land cover types, such as barren or sparsely vegetated, forests, urban, and buildup areas. The mean annual area extent departure of soil freeze/thaw state was greater than the mean before 1985, and the maximum area was up to 0.05×10^6 km^2. It was below the long-term mean after 1985, and the minimum departure was as low as -0.05×10^6 km^2. The mean annual area extent departure of soil CF state exhibited large interannual variability for cropland and grassland types. The mean annual area extent departure of soil PF state ranges $\pm 0.05 \times 10^6$ km^2. For soil UF state, variability opposite to that of soil CF state was found.

Based on mean area extent of soil freeze/thaw state for the six land cover types, the MAAT departure in different land cover types was calculated. Figure 10 indicates warming trends, statistically significant from 1950 to 2010 for every land cover type. The warming rate of MAAT was 0.22°C/decade for barren/sparsely vegetated areas, 0.12°C/decade for forests, 0.16°C/decade for croplands, 0.19°C/decade for grasslands, 0.25°C/decade for permanent wetlands, and 0.18°C/decade for urban and builtup areas, consistent with previous research. This is likely due to the surface energy transfer into the atmosphere by latent heat or sensible heat [*Yang et al*., 2009]. Across China, the overall warming rate was 0.18°C/decade during 1950–2010. Thus, the consistent MAAT warming trend is a potential reason for the observed changes of freeze/thaw state and will therefore be assessed next.

3.5. Relationship Between Air Temperature and FTC

Air temperature likely exhibits the most direct influence on the soil freeze/thaw state, and the relationships between air temperature and FTC are therefore presented here. Figure 11 shows the MAAT changed statistically significantly based on more than 800 sites across China from 1967 to 2013. We find a trend of 0.29 ± 0.03°C/decade, or a statistically significant net change of 1.36°C for the 47 year period. In addition to this overall long-term increase, the time series also indicates some interesting positive and negative departures. Based on the objective change-point analysis, there was no change in MAAT until 1983, followed by a sharp increase of 0.75°C/decade until 1998. From 1999 to 2006, MAAT indicates little change. A sharp decrease of

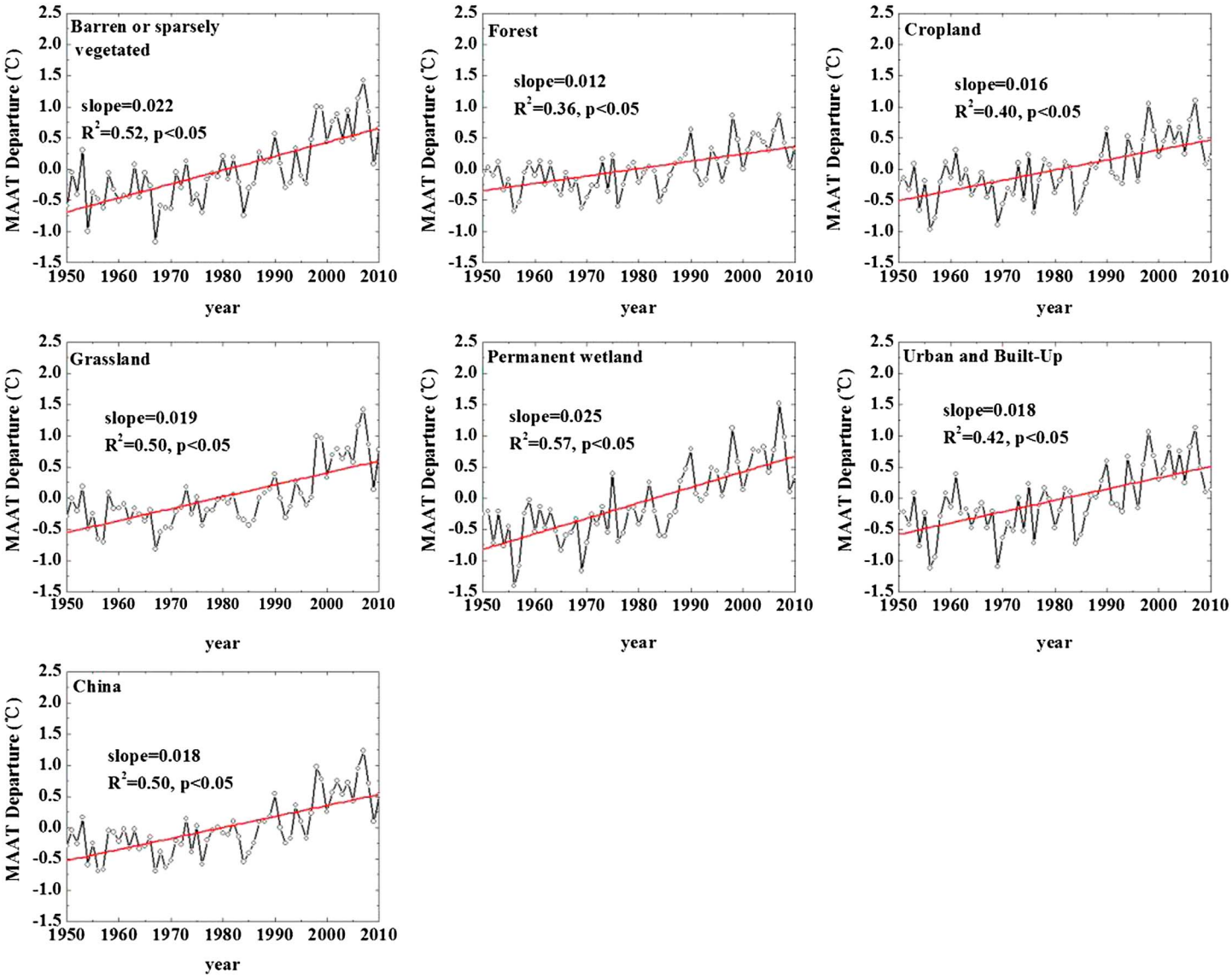

Figure 10. Linear trend of MAAT departures (black line, open black circles) during 1967–2013 based on all available stations across China. Included also is the overall significant trend (black bold line), 1984–1998 trend (red bold line), and 2007–2012 trend (blue bold line).

MAAT appears from 2007 to 2012, at −1.8°C/decade. Thus, the overall 1967–2013 change is largely driven by the increase during 1984–1998 period.

Figure 12 presents the linear trend of FTC and the relationship between FTC and MAAT during 1967–2013. Overall, FTC decreased statistically significantly across China, at a rate of about -0.39 ± 0.05 cycles/decade. The significant correlation coefficient between the FTC and MAAT is −0.65, indicating that 42% of the variance in FTC can be accounted for by changes in MAAT. The negative correlation illustrates that as air temperatures increased, FTC decreased from 1967 to 2013.

4. Discussion

In this research, we analyzed temperature changes and soil freeze/thaw status across China. Compared with previous studies [*Wang et al.*, 2015; *Henry*, 2007; *Jin et al.*, 2015; *Kim et al.*, 2011, 2012; *Kimball and McDonald*, 2008], we found similar temperature changes. But this is the first study to quantify changes in areal extent, including for different land cover classes, of the seasonal soil freeze/thaw status in China.

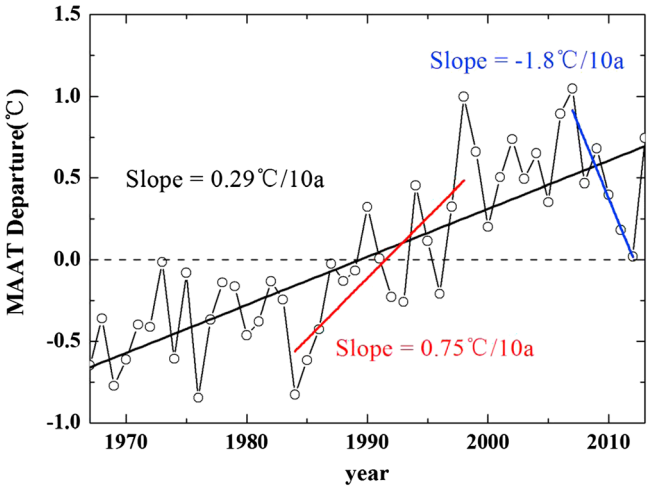

Figure 11. Linear trend of FTC departure and relationship between MAAT and FTC from 1967 to 2013 based on available stations across China.

IPCC AR5 indicates that the global average combined land and ocean surface temperature rose about 0.85°C over the period 1880 to 2012 [*Stocker et al*., 2014]. *Chen and Frauenfeld* [2014] reported that surface air temperature increased by 0.45°C across China during the twentieth century based on 20 Coupled Model Intercomparison Project (Phase 5) models, especially in the Tibetan Plateau region where a stronger increase of 0.54°C was found [*Chen and Frauenfeld*, 2014]. In our research, we combined all available observing sites and found that the greatest positive trends are also for stations located on the Tibetan Plateau (not shown), of similar magnitude as reported in *Frauenfeld et al*. [2005]. Except for this region of accelerated warming, temperature rise was also observed in many other regions [*Li and Zhao*, 2011; *Han et al*., 2013; *Zhao et al*., 2013]. Combined with all available sites, MAAT increased statistically significantly by 0.29°C/decade across China from 1967 to 2013, consistent with *Piao et al.* [2010].

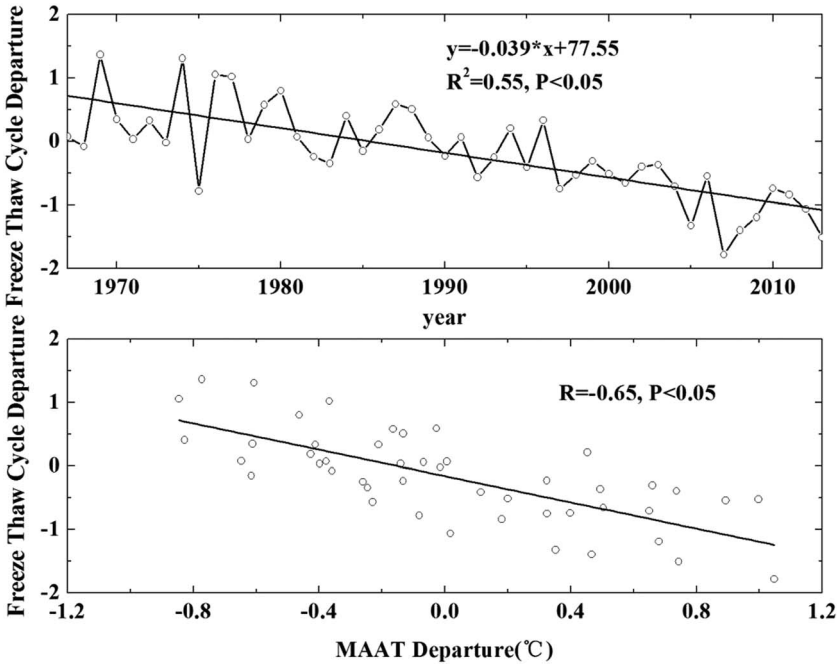

Figure 12. Rate of changes in monthly area extent in seasonal soil freeze/thaw states (CF, PF, and UF) at 5 cm soil depth from 1950 to 2010 across China.

FTC changed statistically significantly at a rate of −0.39 from 1967 to 2013 across China (Figure 11). Similar results have also been found in other regions [*Wang and Zhang*, 2013; *Zhang et al*., 2014; *Li et al*., 2012; *Henry*, 2007; *Anandhi et al*., 2013]. However, other factors such as soil carbon and nutrient losses could also influence the FTC [*Schimel and Clein*, 1996; *Larsen et al*., 2002; *Yanai et al*., 2004], although soil microorganisms may be relatively insensitive to FTC in some systems [*Grogan et al*., 2004].

Generally, greenhouse gases play an important role in global warming; however, the impact of landscape changes must also be assessed. In some cases, the influence of variations in land cover contributes more to climate warming than greenhouse gases [*Gao et al*., 2007; *Lawrence and Chase*, 2010]. We estimated the seasonal soil freeze/thaw state in different land cover types and found that the area extent of CF decreased and increased for UF during 1950–2010 (Figure 7). However, the area extent of PF state increased from November to March and decreased in the other months. Possible explanations are that in winter, rising temperature forced the soil CF state to transition to the PF state, and resulted in the increasing area extent of soil PF state. In summer, the air temperature was already relatively high, and the soil was therefore mainly in the UF state. However, there were still some areas under a PF state where the temperature was really low. With a temperature rise, some soil PF areas developed into the UF state, which means the area extent of soil PF state decreased in summer. Few studies have reported the soil freeze/thaw state at a monthly resolution, although similar results were also found for the Qilian Mountains in the northeastern Tibetan Plateau, where permafrost is present and the MAAT was about −2°C [*Peng et al*., 2013].

Given a temperature rise, the seasonal soil freeze/thaw state is important for ecosystems, hydrological processes, and the carbon cycle. The FTC of near-surface soils influences the ground thermal and hydrologic characteristics, which have a significant impact on the surface energy and moisture balance. Considering the difference in thermal conductivity between frozen and unfrozen soil, changes of freeze/thaw state affect soil heat flux significantly. In addition, frozen soil water reduces the hydraulic conductivity, leading to either more runoff due to decreased infiltration or higher soil moisture content due to restricting drainage [*Zhang et al*., 2001].

5. Summary and Conclusions

This study analyzed the response of changes in seasonal soil freeze/thaw to temperature change from 1950 to 2010 in China concurrent with 1967–2013 air and ground temperature changes. We investigated seasonal soil freeze/thaw area extent changes and also establish the connections between air temperature and FTC. The main conclusions can be summarized as follows:

1. Temperature increases across China have been significant in the past 47 years. The warming trend was different for different time periods and in different regions. The increase in MAAT on the Tibetan Plateau was higher than in other areas. There was an overall statistically significant increase of 0.29 ± 0.03°C/decade from 1967 to 2013. However, a sharp increasing MAAT trend of 0.75°C/decade is evident from 1984 to 1998.
2. From 1967 to 2013, there was decrease trend in FTC, at a statistically significant rate of −0.39 ± 0.05 cycles/decade. Furthermore, a negative correlation between FTC and MAAT was evident across China.
3. Based on the relationship between monthly air temperature and monthly soil freeze days, we divide the temperature range of the soil freeze/thaw states into three types, CF, PF, and UF in different cover types. The temperature range of soil freeze/thaw state is between −7 and 6°C in barren/sparsely vegetated areas, between −9 and 4°C in forests, between −6.5 and 5°C in croplands, between −8 and 4°C in grasslands, between −6 and 3.5°C in permanent wetlands, and between −7 and 6°C for urban areas.
4. Changes in area extent of seasonal soil freeze/thaw state are somewhat different and complicated compared to temperature trends. The mean annual area extent of soil CF state decreased statistically significantly at a rate of -0.043×10^6 km^2/decade from 1950 to 2010. For the soil UF state, the mean annual area extent increased significantly by about 0.037×10^6 km^2/decade. However, the mean annual area extent of soil PF state increased statistically significantly by 0.032×10^6 km^2/decade from 1950 to 1993 and exhibited no change from 1993 to 2010.
5. The monthly area extent of CF state decreased statistically significantly for all months of the year but decreased significantly for the UF state. The PF state showed a complex pattern, increasing during the cold season (November–March) and decreasing in the other months.

6. During 1950–2010, the freeze status value decreased statistically significantly from winter to summer and increased from spring to summer. The fraction value was larger in summer than in winter. Spatially, the maximum status value was mainly located in the south of China. The minimum value was in the north of China and on the Tibetan Plateau.

These findings have implications for engineering applications, livestock, and agriculture in China. A temperature rise will further reduce the CF area extent, and increase the area of PF, and UF state, which can promote plant growth. Seasonal soil freeze/thaw state is one of the most fundamental characteristics for estimating seasonally frozen ground. Thus, the results will be useful to advance understanding of seasonally frozen ground dynamics, such as the impacts to ecosystems and hydrological processes.

Acknowledgments
This study was funded by the National Natural Science Foundation of China (grant 91325202), the National Key Scientific Research Program of China (grant 2013CBA01802), and the Fundamental Research Funds for the Central Universities (lzujbky-2015-217 and lzujbky-2015-215). We appreciate the thoughtful input from three anonymous reviewers and the Editor, whose comments improved this manuscript. The land cover data were obtained from the Environmental and Ecological Science Data Center for West China (http://westdc.westgis.ac.cn/). We acknowledge computing resources and time at the Supercomputing Center of Cold and Arid Region Environment and Engineering Research Institute of Chinese Academy of Sciences.

References

Anandhi, A., P. Sriram, P. H. Gowda, M. Knapp, S. Hutchinson, J. Harrington, L. Murray, M. B. Kirkham, and C. W. Rice (2013), Long-term spatial and temporal trends in frost indices in Kansas, USA, *Clim. Change*, *120*, 169–181, doi:10.1007/s10584-013-0794-4.

Bates, B. C., R. E. Chandler, and A. W. Bowman (2012), Trend estimation and change point detection in individual climatic series using flexible regression methods, *J. Geophys. Res.*, *117*, D16106, doi:10.1029/2011JD017077.

Chen, F., H. Lin, W. Zhou, T. Hong, and G. Wang (2013), Surface deformation detected by ALOS PALSAR small baseline SAR interferometry over permafrost environment of Beiluhe section, Tibet Plateau, China, *Remote Sens. Environ.*, *138*, 10–18, doi:10.1016/j.rse.2013.07.006.

Chen, L., and O. W. Frauenfeld (2014), Surface air temperature changes over the twentieth and twenty-first centuries in China simulated by 20 CMIP5 models, *J. Clim.*, *27*, 3920–3937, doi:10.1175/JCLI-D-13-00465.1.

Frauenfeld, O. W., and T. Zhang (2011), An observational 71-year history of seasonally frozen ground changes in the Eurasian high latitudes, *Environ. Res. Lett.*, *6*, 044024, doi:10.1088/1748-9326/6/4/044024.

Frauenfeld, O. W., T. Zhang, R. G. Barry, and D. Gilichinsky (2004), Interdecadal changes in seasonal freeze and thaw depths in Russia, *J. Geophys. Res.*, *109*, D05101, doi:10.1029/2003JD004245.

Frauenfeld, O. W., T. Zhang, and M. C. Serreze (2005), Climate change and variability using European Centre for Medium-Range Weather Forecasts Reanalysis (ERA-40) temperatures on the Tibetan Plateau, *J. Geophys. Res.*, *110*, D02101, doi:10.1029/2004JD005230.

Gao, X., D. Zhang, Z. Chen, J. S. Pal, and F. Giorgi (2007), Land use effects on climate in China as simulated by a regional climate model, *Sci. China Ser. D Earth Sci.*, *37*, 397–404, doi:10.1007/s11430-007-2060-y.

Grogan, P., A. Michelsen, P. Ambus, and S. Jonasson (2004), Freeze–thaw regime effects on carbon and nitrogen dynamics in sub-arctic heath tundra mesocosms, *Soil Biol. Biochem.*, *36*, 641–654, doi:10.1016/j.soilbio.2003.12.007.

Gruber, S., and W. Haeberli (2007), Permafrost in steep bedrock slopes and its temperature-related destabilization following climate change, *J. Geophys. Res.*, *112*, F02S18, doi:10.1029/2006JF000547.

Guo, D., M. Yang, and H. Wang (2011), Characteristics of land surface heat and water exchange under different soil freeze/thaw conditions over the central Tibetan Plateau, *Hydrol. Processes*, *25*, 2531–2541, doi:10.1002/hyp.8025.

Han, C. H., Z. X. Hao, and J. Y. Zheng (2013), Regionalization of temperature changes in China and characteristics of temperature in different regions during 1951–2010, *Prog. Geogr.*, *32*, 887–896, doi:10.11820/dlkxjz.2013.06.005.

Hayashi, M., G. van der Kamp, and R. Schmidt (2003), Focused infiltration of snowmelt water in partially frozen soil under small depressions, *J. Hydrol.*, *270*, 214–229, doi:10.1016/S0022-1694(02)00287-1.

Henry, H. A. (2007), Climate change and soil freezing dynamics: Historical trends and projected changes, *Clim. Change*, *87*, 421–434, doi:10.1007/s10584-007-9322-8.

Jin, R., and X. Li (2002), A review on the algorithms of frozen/thaw boundary detection by using passive microwave remote sensing, *Rem. Sens. Technol. Appl.*, *17*, 370–375.

Jin, R., T. Zhang, X. Li, X. Yang, and Y. Ran (2015), Mapping surface soil freeze-thaw cycles in China based on SMMR and SSM/I brightness temperatures from 1978–2008, *Arct. Antarct. Alp. Res.*, *47*, 213–229, doi:10.1657/AAAR00C-13-304.

Jin Rui, L. X., and C. Tao (2009), A decision tree algorithm for surface freeze/thaw classification using SSM/I, *J. Remote Sens.*, *01*, 152–161.

Jorgenson, M. T., Y. L. Shur, and E. R. Pullman (2006), Abrupt increase in permafrost degradation in Arctic Alaska, *Geophys. Res. Lett.*, *33*, L02503, doi:10.1029/2005GL024960.

Kim, Y., J. S. Kimball, K. C. McDonald, and J. Glassy (2011), Developing a global data record of daily landscape freeze/thaw status using satellite passive microwave remote sensing, *IEEE Trans. Geosci. Remote Sens.*, *49*, 949–960, doi:10.1109/TGRS.2010.2070515.

Kim, Y., J. S. Kimball, K. Zhang, and K. C. McDonald (2012), Satellite detection of increasing Northern Hemisphere non-frozen seasons from 1979 to 2008: Implications for regional vegetation growth, *Remote Sens. Environ.*, *121*, 472–487, doi:10.1016/j.rse.2012.02.014.

Kimball, J. S., and K. C. McDonald (2008), An Earth system data record for land surface freeze/thaw state: Quantifying terrestrial water mobility constraints to global ecosystem processes, *In AGU Fall Meeting Abstracts*, 05.

Kuchment, L. S., A. N. Gelfan, and V. N. Demidov (2000), A distributed model of runoff generation in the permafrost regions, *J. Hydrol.*, *240*, 1–22, doi:10.1016/S0022-1694(00)00318-8.

Larsen, K. S., S. Jonasson, and A. Michelsen (2002), Repeated freeze–thaw cycles and their effects on biological processes in two arctic ecosystem types, *Appl. Soil Ecol.*, *21*, 187–195, doi:10.1016/S0929-1393(02)00093-8.

Lawrence, P. J., and T. N. Chase (2010), Investigating the climate impacts of global land cover change in the community climate system model, *Int. J. Climatol.*, *30*, 2066–2087, doi:10.1002/joc.2061.

Legates, D. R., and C. J. Willmott (1990), Mean seasonal and spatial variability in global surface air temperature, *Theor. Appl. Climatol.*, *41*, 11–21, doi:10.1007/BF00866198.

Li, X., R. Jin, X. Pan, T. Zhang, and J. Guo (2012), Changes in the near-surface soil freeze–thaw cycle on the Qinghai-Tibetan Plateau, *Int. J. Appl. Earth Obs.*, *17*, 33–42, doi:10.1016/j.jag.2011.12.002.

Li, Y., and X. Zhao (2011), Surface air temperature changes of different land cover types in China during 1979–2007, *Acta Sci. Nat. Univ. Pekinensis*, *47*, 1129–1136.

Liu, L., T. Zhang, and J. Wahr (2010), InSAR measurements of surface deformation over permafrost on the North Slope of Alaska, *J. Geophys. Res.*, *115*, F03023, doi:10.1029/2009JF001547.

Liu, L., K. Schaefer, T. Zhang, and J. Wahr (2012), Estimating 1992–2000 average active layer thickness on the Alaskan North Slope from remotely sensed surface subsidence, *J. Geophys. Res.*, *117*, F01005, doi:10.1029/2011JF002041.

McGuire, A. D., C. Wirth, M. Apps, J. Beringer, J. Clein, H. Epstein, and D. Efremov (2002), Environmental variation, vegetation distribution, carbon dynamics and water energy exchange at high latitudes, *J. Veg. Sci.*, *13*, 301–314, doi:10.1111/j.1654-1103.2002.tb02055.x.

McNamara, J. P., D. L. Kane, and L. D. Hinzman (1998), An analysis of streamflow hydrology in the Kuparuk River Basin, arctic Alaska a nested watershed approach, *J. Hydrol.*, *206*, 39–57, doi:10.1016/S0022-1694(98)00083-3.

Miyazaki, S., M. Ishikawa, N. Baatarbileg, S. Damdinsuren, N. Ariuntuya, and Y. Jambaljav (2014), Interannual and seasonal variations in energy and carbon exchanges over the larch forests on the permafrost in northeastern Mongolia, *Polar Sci.*, *8*, 166–182, doi:10.1016/j.polar.2013.12.004.

Mu, C., T. Zhang, Q. Wu, X. Peng, B. Cao, X. Zhang, and G. Cheng (2015), Editorial: Organic carbon pools in permafrost regions on the Qinghai–Xizang (Tibetan) Plateau, *Cryosphere*, *9*, 479–486, doi:10.5194/tc-9-479-2015.

Peng, X., T. Zhang, and X. Pan (2013), Spatial and temporal variations of seasonally frozen ground over the Heihe River Basin of Qilian Mountain in western China, *Adv. Earth Sci.*, *28*, 497–508.

Peng, X., O. W. Frauenfeld, T. Zhang, K. Wang, B. Cao, X. Zhong, H. Su, and C. Mu (2016), Response of seasonal soil freeze depth to climate change across China, *Cryosphere*, doi:10.5194/tc-2016-129.

Peterson, T. C., and R. S. Vose (1997), An overview of the Global Historical Climatology Network temperature database, *Bull. Am. Meteorol. Soc.*, *78*, 2837–2849.

Peterson, T. C., R. S. Vose, R. Schmoyer, and V. Razuvaëv (1998), Global historical climatology network (GHCN) quality control of monthly temperature data, *Int. J. Climatol.*, *18*, 1169–1179.

Piao, S., P. Ciais, Y. Huang, Z. Shen, S. Peng, J. Li, and P. Friedlingstein (2010), The impacts of climate change on water resources and agriculture in China, *Nature*, *467*(7311), 43–51.

Ran, Y., X. Li, and L. Lu (2010), Evaluation of four remote sensing based land cover products over China, *Int. J. Remote Sens.*, *31*, 391–401, doi:10.1080/01431160902893451.

Schimel, J. P., and J. S. Clein (1996), Microbial response to freeze–thaw cycles in tundra and taiga soils, *Soil Eiot. Biorhem*, *28*, 1061–1066, doi:10.1016/0038-0717(96)00083-1.

Schuur, E. A., J. G. Vogel, K. G. Crummer, H. Lee, J. O. Sickman, and T. E. Osterkamp (2009), The effect of permafrost thaw on old carbon release and net carbon exchange from tundra, *Nature*, *459*, 556–9, doi:10.1038/nature08031.

Sinha, T., and K. A. Cherkauer (2008), Time series analysis of soil freeze and thaw processes in Indiana, *J. Hydrometeorol.*, *9*, 936–950, doi:10.1175/2008JHM934.1.

Smith, N. V. (2004), Trends in high northern latitude soil freeze and thaw cycles from 1988 to 2002, *J. Geophys. Res.*, *109*, D12101, doi:10.1029/2003JD004472.

Song, C., X. Wang, Y. Miao, J. Wang, R. Mao, and Y. Song (2014), Effects of permafrost thaw on carbon emissions under aerobic and anaerobic environments in the Great Hing'an Mountains, China, *Sci. Total Environ.*, *487*, 604–10, doi:10.1016/j.scitotenv.2013.09.083.

Stocker, T. F., D. Qin, G. K. Plattner, M. Tignor, S. K. Allen, J. Boschung, and B. M. Midgley (2014), *Climate Change 2013: The Physical Science Basis*, Cambridge Univ. Press, Cambridge, U. K., and New York.

Streletskiy, D., A. Sherstiukov, O. W. Frauenfeld, and F. E. Nelson (2015), Changes in the 1963–2013 shallow ground thermal regime in Russian permafrost regions, *Environ. Res. Lett.*, *10*(11, 125005), doi:10.1088/1748-9326/10/12/125005.

Tarnocai, C., J. G. Canadell, E. A. G. Schuur, P. Kuhry, G. Mazhitova, and S. Zimov (2009), Soil organic carbon pools in the northern circumpolar permafrost region, *Global Biogeochem. Cycles*, *23*, GB2023, doi:10.1029/2008GB003327.

Wang, G., H. Hu, and T. Li (2009), The influence of freeze–thaw cycles of active soil layer on surface runoff in a permafrost watershed, *J. Hydrol.*, *375*, 438–449, doi:10.1016/j.jhydrol.2009.06.046.

Wang, G., T. Mao, J. Chang, and J. Du (2014), Impacts of surface soil organic content on the soil thermal dynamics of alpine meadows in permafrost regions: Data from field observations, *Geoderma*, *232*, 414–425, doi:10.1016/j.geoderma.2014.05.016.

Wang, K., and T. Zhang (2013), Spatial and temporal distribution and variations in the near-surface soil freezing days across China, 1956–2006, *Adv. Earth Sci.*, *11*, 1269–1275.

Wang, K., T. Zhang, and X. Zhong (2015), Changes in the timing and duration of the near-surface soil freeze/thaw status from 1956 to 2006 across China, *Cryosphere*, *9*, 1321–1331, doi:10.5194/tc-9-1321-2015.

Way, J., E. J. Rignot, K. C. McDonald, R. Oren, R. Kwok, G. Bonan, and J. E. Roth (1994), Evaluating the type and state of Alaska taiga forests with imaging radar for use in ecosystem models, *IEEE Trans. Geosci. Remote Sens.*, *32*, 353–370, doi:10.1109/36.295050.

Willmott, C. J., and K. Matsuura (1995), Smart interpolation of annually averaged air temperature in the United States, *J. Appl. Meteorol.*, *34*, 2577–2586.

Willmott, C. J., and S. M. Robeson (1995), Climatologically aided interpolation (CAI) of terrestrial air temperature, *Int. J. Climatol.*, *15*, 221–229, doi:10.1002/joc.3370150207.

Willmott, C. J., C. M. Rowe, and W. D. Philpot (1985), Small scale climate maps a sensitivity analysis of some common assumptions associated with grid-point interpolation and contouring, *Am. Cartogr.*, *12*, 5–16, doi:10.1559/152304085783914686.

Yamazaki, Y., J. Kubota, T. Ohata, V. Vuglinsky, and T. Mizuyama (2006), Seasonal changes in runoff characteristics on a permafrost watershed in the southern mountainous region of eastern Siberia, *Hydrol. Processes*, *20*, 453–467, doi:10.1002/hyp.5914.

Yanai, Y., K. Toyota, and M. Okazaki (2004), Effects of successive soil freeze–thaw cycles on soil microbial biomass and organic matter decomposition potential of soils, *Soil Sci. Plant Nutr.*, *50*, 821–829, doi:10.1080/00380768.2004.10408542.

Yang, X., Y. Zhang, L. Liu, W. Zhang, M. Ding, and Z. Wang (2009), Sensitivity of surface air temperature change to land use/cover types in China, *Sci. China Ser. D: Earth Sci.*, *52*, 1207–1215, doi:10.1007/s11430-009-0085-0.

Zhang, L., S. Zhao, and L. Jiang (2009), The time series of microwave radiation from representative land surfaces in the upper reaches of Heihe River during alternation of freezing and thawing, *J. Glaciol. Geocryol.*, *31*, 198–206.

Zhang, L., J. Lingmei, L. Chai, S. S. Zhao, T. Zhao, and X. Li (2011), Research advances in passive microwave remote sensing of freeze-thaw processes over complex landscapes, *Adv. Earth Sci.*, *26*, 1023–1029.

Zhang, T., and R. L. Armstrong (2001), Soil freeze/thaw cycles over snow-free land detected by passive microwave remote sensing, *Geophys. Res. Lett.*, *28*, 763–766, doi:10.1029/2000GL011952.

Zhang, T., R. Barry, D. Gilichinsky, S. Bykhovets, V. Sorokovikov, and J. Ye (2001), An amplified signal of climatic change in soil temperatures during the last century at Irkutsk, Russia, *Clim. Change*, *49*, 41–76, doi:10.1023/A:1010790203146.

Zhang, T., R. Armstrong, and J. Smith (2003), Investigation of the near-surface soil freeze-thaw cycle in the contiguous United States: Algorithm development and validation, *J. Geophys. Res.*, *108*(D22), 8860, doi:10.1029/2003JD003530.

Zhang, T., R. G. Barry, and R. L. Armstrong (2004), Application of satellite remote sensing techniques to frozen ground studies, *Polar Geogr.*, *28*, 163–196, doi:10.1080/789610186.

Zhang, T., O. W. Frauenfeld, M. C. Serreze, A. Etringer, C. Oelke, J. McCreight, R. G. Barry, D. Gilichinsky, D. Yang, and H. Ye (2005), Spatial and temporal variability in active layer thickness over the Russian Arctic drainage basin, *J. Geophys. Res.*, *110*, D16101, doi:10.1029/2004JD005642.

Zhang, T., R. Jin, and F. Gao (2009), Overview of the satellite remote sensing of frozen ground: Passive microwave sensors, *Adv. Earth Sci.*, *24*, 1073–1083.

Zhang, X., S. Xu, C. Li, L. Zhao, H. Feng, G. Yue, and G. Cheng (2014), The soil carbon/nitrogen ratio and moisture affect microbial community structures in alkaline permafrost-affected soils with different vegetation types on the Tibetan plateau, *Res. Microbiol.*, *165*, 128–39, doi:10.1016/j.resmic.2014.01.002.

Zhao, S. J., L. X. Zhang, Y. P. Zhang, L. M. Jiang, W. B. Xing, and T. J. Zhao (2009), The coherent microwave emission of freezing soil: Experimental research and model simulation, *Proc. Geosci. Remote Sens. Symp.*, *2*, 678–681, doi:10.1109/IGARSS.2009.5418179.

Zhao, T., L. Chen, and Z. Ma (2013), Simulation of historical and projected climate change in arid and semiarid areas by CMIP5 models, *Chin. Sci. Bull.*, *59*, 412–429.

Zimov, S. A., E. A. Schuur, and F. S. Chapin III (2006), Permafrost and the global carbon budget, *Science*, *312*, 1612–3.